Short Communication

Topographic control on the recession of the Kokthang glacier and its effect on proglacial lake dynamics

Priyom Roy[1] · Swati Singh[1] · K. Vinod Kumar[1]

Received: 9 July 2020 / Accepted: 15 October 2020 / Published online: 12 November 2020

Abstract
We present the preliminary observations about the recession and resultant lake formation of the Kokthang glacier in Sikkim, India. We have analyzed time-series satellite imagery from Corona and Landsat satellites over a span of 55 years to delineate the uncharacteristic recession and its control on the proglacial lake formation. It is seen that the eastern tributary of the glacier has melted and receded at ~ 37 m/yr between 1989 and 2000, which is twice as fast as its western counterpart (~ 18 m/yr). The water spread of the proglacial lake has increased from ~ 11.8 ha to ~ 38.5 ha between 1962 and 2017 with commensurate volume change. The underlying topographic slope possibly controls the differential recession of the tributaries, wherein the eastern slope is significantly steeper (~ 44°) than the western slope (~ 20°). The variation of the slope may have resulted in the differential thickness of ice accumulation (estimated by empirical slope thickness relationship). The eastern tributary is estimated to be less thick than its western counterpart and thus has receded faster.

Keywords Kokthang glacier · Proglacial lake · Recession · Landsat imagery

1 Introduction

The change in global climatic conditions in the past half a century has significantly changed the distribution and extent of glaciers, especially in the Himalaya. Most of these Himalayan glaciers have demonstrated quantifiable retreat [1–3]. The annual rates of the recession of Himalayan glaciers are estimated to be around 16–35 m [3–5]. Though the recession of the glaciers is primarily controlled by climate change, it also depends upon several non-climatic factors such as topography and debris cover [6]. Field studies of glaciers of the Himalayas are constrained due to the inaccessible and challenging terrain, thus making remote sensing methods important [7]. Measurement of recession rates based on temporal remote sensing imagery is an area of active research across the world [7–9]

The associated proglacial lakes, which are generally a consequence of such recession, in some instances, are now presenting a threat to the establishments downstream with the possibility of a moraine breach and glacial lake outburst flood. Such incidents have been reported across the glaciated higher reaches of the Himalayas. A breach of a glacial lake in Nepal Tibet border in July 1981 caused severe economic losses, which included complete inundation of the Sunkoshi Hydroelectric power station [10]. Similarly, another incident was also reported from Karakoram Himalayas in June 2008 [11] and Luggye Tso in Bhutan on October 6, 1994 [12]. In India, recently, the large-scale disaster in Kedarnath was partly attributed to the breach of a moraine-dammed glacial lake [13]. These incidents have triggered the identification and monitoring of the glacier and associated glacial lakes. Comprehensive inventories of glacial lakes have been created for all the

✉ Priyom Roy, roy.priyom@gmail.com | [1]Geosciences Group, National Remote Sensing Centre, Indian Space Research Organization, Hyderabad 500037, India.

significant glaciers in the Sikkim Himalayas [1] and for the North-Western Himalayas [14].

The Kokthang glacier is a small yet significant glacier located on the eastern boundary of the Sikkim state in India (Fig. 1a). In this study, we present a preliminary analysis of the glacier using satellite-based remote sensing data [15–18]. We have estimated the recession rates of the two tributaries of the glacier and the change in water spread of the lake associated with it. We have made an approximate estimate of the temporal volume change of the lake using an empirical volume area relationship [19]. We have also presented a plausible reason for the uncharacteristic recession of the two tributaries of the glacier. The underlying topographic variation between the eastern and western tributary and the consequently accumulated ice thickness may have resulted in the eastern tributary to recede at a faster rate [20].

2 Study area

The state of Sikkim, comprising 0.5 percent of India's landmass, has 84 glaciers, the largest number as compared to any other state or union territory [21]. The Kokthang Glacier originates from the Kokthang peak, a satellite peak south of the Kanchenjunga Massif in Sikkim. It is situated south of the East Rathong Glacier. It is geographically bound by coordinates: 27° 31′ N–27° 34′ N and 88° 04′ E–88° 06′ E. The valley has an average altitude of 5400 m and is surrounded by steep snow-covered peaks. The region lies in the High Himalayan Crystalline zone with high-grade metamorphic gneisses [22]. The climate, in general, is that of dry temperate.

Geomorphologically, the glacier may be described as a valley glacier with an accumulation zone at an altitude of 5000–5400 m. Large number of crevasses can be seen at the margin of the accumulation and ablation zone from satellite imagery. The depositional landforms like lateral moraines (left and right) and terminal moraine are distinct (Fig. 1b). The melt of the glacier forms the proglacial lake with terminal moraine forming the wall in the south. The terminal moraine appears to contain an iced core as few small water bodies can be seen accumulated within the moraine. The outwash plain is formed by the melting glacial ice, from which a tributary drains into the main Rangit river.

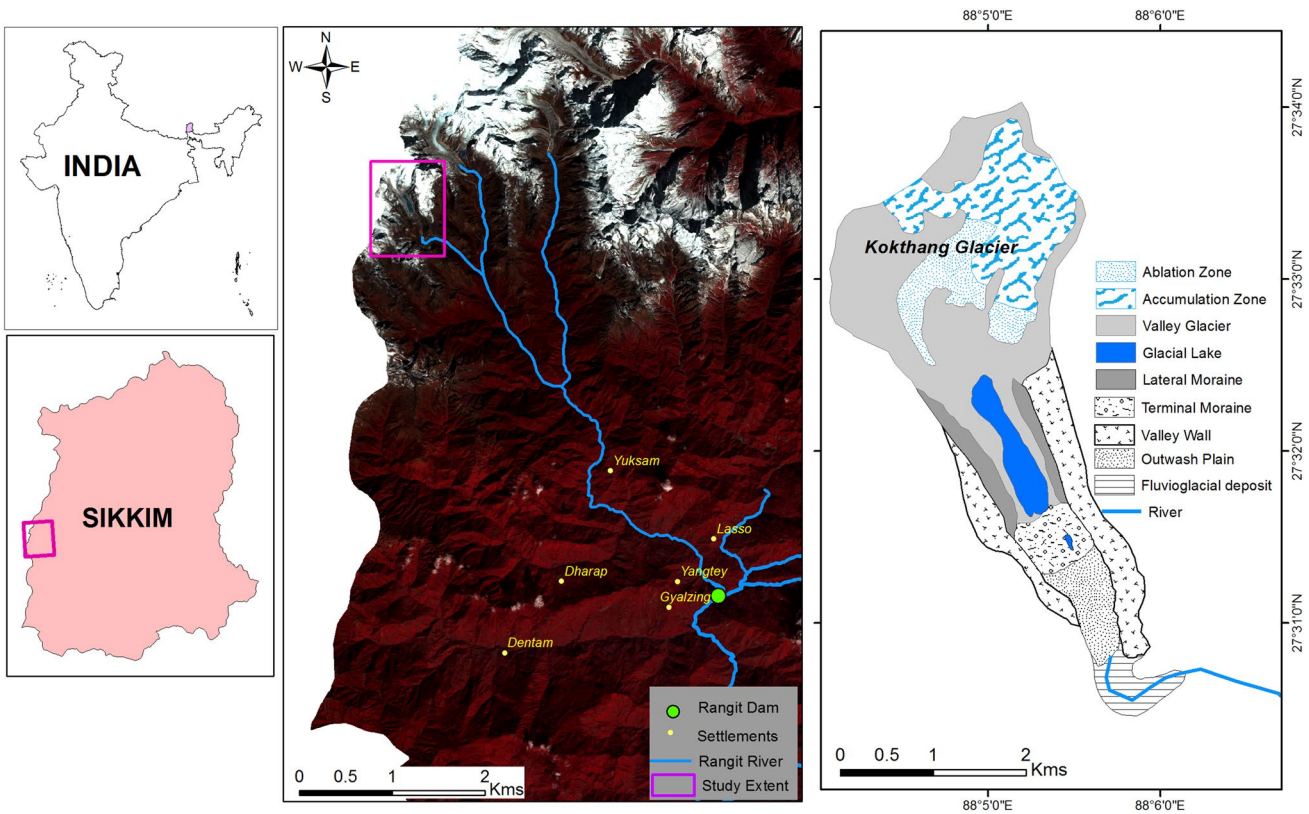

Fig. 1 **a** Position of Kokthang Glacier (demarcated by a pink rectangle), **b** Simplified Geomorphological map of Kokthang Glacier

3 Materials and method

3.1 Analysis of satellite imagery and DEM

We have used time-series satellite imagery from declassified Corona (source: https://earthexplorer.usgs.gov/) and Landsat satellites (source: United States Geological Survey) to analyze the changes occurring over 55 years for the glacier and the proglacial lake formed at the vicinity of the terminus. All the images, except that of the Corona imagery (panchromatic), were preprocessed as per standard steps, including image layer stacking, resolution merge, co-registration and merging (pan-sharpening). To nullify the effect of seasonal variations, we attempted to analyze data of October–December for all the considered years. The variation of the glacial terminus was interpreted using image interpretation keys such as tone, shape and structure from bands 5-4-3 RGB composite Landsat images. In debris-covered glaciers, discrimination of debris and snow/ice from remote sensing imagery remains to be a challenge. We have used band ratios of Landsat bands 4 and 5 (ratio image) to delineate the debris from the ice [23].

Further, as supporting evidence, principal component analysis of the Landsat imageries was also attempted to demarcate the debris and glaciated snow and ice [24]. In addition to this, to extract elevation information to understand glacial recession, Cartosat-1 (source: ISRO) digital elevation model (DEM) of 30 m posting and 8 m vertical accuracy was used. Elevation and slope information from the DEM is used to demarcate the height of the glacial terminus and estimate the along slope movement in order to calculate the approximate recession rate. Further, the slope information is also used to estimate ice thickness, as described in Sect. 3.3. A summary of time-series satellite data used in the study, is provided in Table 1.

3.2 Estimation of lake volume

Estimation of the volume of glacial lakes necessitates specific in situ measurements. However, empirical relations, which relates the water spread area to the volume of the lake, have been postulated by researchers. Huggel et al. presented a volume–area relationship of glacial lakes in the Swiss Alps [19]. In the absence of any other ground information, we use the empirical relation [16] given in Eq. 1 to estimate the volume of the proglacial lake from the water spread area deduced by the interpretation of the satellite imagery. We estimate the volume for all the observations years (1962–2017).

The lake volume,

$$V = 0.104A^{0.42} \quad (1)$$

where V is the lake volume in m^3 and A is the lake area in m^2.

3.3 Estimation of ice thickness from the "slope-dependent method"

The thickness of ice on the glacier is an important parameter to understand glacial dynamics. We estimate the ice thickness from the topographic slope using the "slope-dependent method" presented by Cooper et al. [20]. The ice thickness H, of distribution of the glacier, is given as:

$$H = \tau/(f\rho g \sin\alpha) \quad (2)$$

where τ is the basal shear stress, ρ is the density of ice, g the acceleration due to gravity, f is the shape factor, H is the ice thickness, and α is the surface slope. Here the value of τ used is 1.5 bar, the value of g is ~ 9.81 m/s^2, and the density of ice is taken as 900 kg/m^3 [17]. Here an average value of f = 0.8 is used for the entire glacier [20]. The surface slope α is estimated from the DEM and is measured along with equispaced points along the long axis of the tributary glaciers.

Table 1 Summary of temporal satellite imagery used in the analysis

Image	Acquisition date	Spatial resolution	Bands used
Corona (Declassified)	15-12-1962	7.5 m	Panchromatic
Landsat 2 (Multispectral Scanner)	30-11-1976	80 m	Visible, Near-infrared and Shortwave infrared
Landsat 5 (Thematic Mapper)	31-12-1987	30 m	
Landsat 5 (Thematic Mapper)	05-11-1996	30 m	
Landsat 7 (Enhanced Thematic Mapper Plus)	13-10-2000	30 m	
Landsat 7 (Enhanced Thematic Mapper Plus)	17-12-2006	30 m	
Landsat 8 (Observational Land Imager)	25-11-2017	30 m	

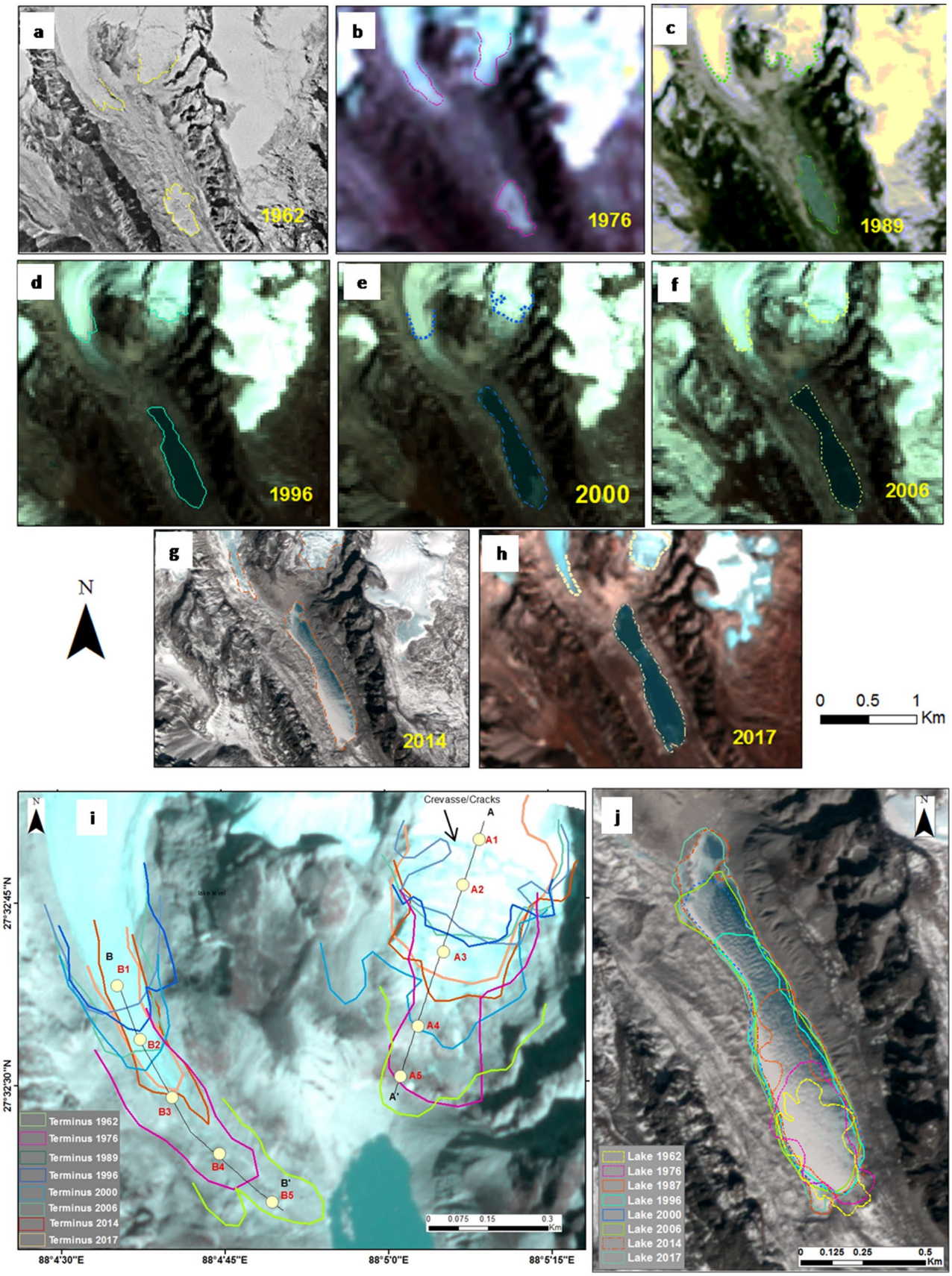
a
1962
b
1976
c
1989
d
1996
e
2000
f
2006
g
2014
h
2017
N
0 0.5 1
Km
i
Crevasse/Cracks
A
A1
A2
A3
A4
A5
A'
B
B1
B2
B3
B4
B'
B5
Terminus 1962
Terminus 1976
Terminus 1989
Terminus 1996
Terminus 2000
Terminus 2006
Terminus 2014
Terminus 2017
0 0.075 0.15 0.3
Km
27°32'45"N
27°32'30"N
88°4'30"E
88°4'45"E
88°5'0"E
88°5'15"E
j
Lake 1962
Lake 1976
Lake 1987
Lake 1996
Lake 2000
Lake 2006
Lake 2014
Lake 2017
0 0.125 0.25 0.5
Km

◂**Fig. 2** **a-h**. Temporal changes in glacier and lake, **i** Change in position of terminus as seen from temporal satellite imagery of Corona and Landsat series. **j** Change in water spread of the lake from 1962 to 2017

4 Results and discussion

The declassified Corona panchromatic imagery of December 1962 was taken as the base data. It is the oldest available imagery of the region and provides a suitable benchmark against which the change detection study can be carried out. In this image, the lake is seen within the valley, dammed against the terminal moraine (Fig. 2a). Though it appears to be completely frozen, the extent of the ice sheet outlining the frozen surface represents the lake area. The primary glacier (western valley) and the tributary glacier (eastern valley) are significantly snow-covered (in October and November). As seen from the Landsat imagery, between 1976 and 1989 (Fig. 2b and c), the glaciers have observably receded with the lake occupying a more considerable areal extent in 1989 (Fig. 2c). In 1996 and 2000 imagery (Fig. 2d and e), it is seen that the lake has elongated along its long axis and the eastern tributary glacier has receded, almost to a hanging valley with significant crevasses near the terminus. In 2006 and 2014 (Fig. 2f and g), a further lengthwise extension of the lake is seen. Finally, in 2017, it appears that both the contributing glaciers have receded away from the lake. Presently, it appears that the lake is in a steady-state with no change in the area of the water spread.

We have analyzed the quantitative change in the position of the terminus (tongue) (Fig. 2i) vis-a-vis the change in lake area (Fig. 2j) using the Cartosat-1 DEM. The mean slope of the eastern tributary is ~ 44°, whereas that of the western tributary is around ~ 20°. It is seen that between 1962 and 1989, the position of the terminuses has gradually receded (Fig. 2i). The terminus of the western tributary has receded from an elevation of 4850 m in 1962 to an elevation of 4960 m in 1989 and further to an elevation of 5030 m in 2000. This translates to an along with slope recession (using triangulation) of ~ 320 m and ~ 205 m, thus deriving a rate of ~ 12 m/yr and ~ 18 m/y between the observation years. Whereas, the terminus of it is eastern counterpart has receded from an elevation of 4865 m to 5000 m between 1962 and 1989 and further to a height 5290 m in the year 2000. This equates to an along slope recession of ~ 191 m and ~ 410 m respectively, thus deriving a rate of ~ 7 m/yr and ~ 37 m/y between the observation years. Between 1962 and 1989, both the tributaries have receded at a similar rate (Fig. 3) with a commensurate change in the lake area, measured to be around 11.8 ha (Fig. 2j). After that, there has been a significant recession of both the tributaries leading to the expansion of the lake. From an aerial extent of 17.6 Ha in 1989, the area has increased to 32.4 ha in 2006 and further to the extent of 38.5 ha in 2017. The commensurate increase in the volume of the lake (calculated using Eq. 1) is from 1.6×10^6 m^3 in 1969 to 2.9×10^6 m^3 in 1989 and 8.6×10^6 m^3 in 2014 (Fig. 3a). As the estimates of the recession rate suggest that the eastern tributary has receded at a faster rate. Therefore, the melt from the eastern tributary may have primarily contributed to the expansion of the lake. Post-2006, it is observed that there have been fluctuations in the position of the terminus, especially of the eastern tributary. This may be attributed to the opening up of the crevasses and gravitational downslope movement of the glacier. However, the complete disconnection of the glaciers with the lake is noticed between 2014 and 2017 and has reduced the supply of meltwater to the same. Hence, the lake area seems to be static with minor variation between 2014 and 2017.

The area of the lake appears to be stable in the last five years, and it seems that there may not be any possible increase in the water spread of the lake as the core ice of the moraines of the receded glaciers gradually melts. However, the asymmetric recession of the two contributing tributary glaciers to the lake dynamics indicates some associated geomorphic/topographic control (Fig. 3a). Further, both the tributaries are similar in their quantum of debris cover and are southeast facing; hence 'slope-aspect' or debris cover effect is nullified. However, as discussed earlier the eastern glacier is situated on a much steeper slope of ~ 44° than the western counterpart (~ 20°). This may probably imply that the variation of the underlying topography has control over the recession rate of the glacier in this region (Fig. 3b). Such topographic control has been earlier reported for Himalayan glaciers [9, 21].

It has also been observed that small and steeply sloping glaciers recess faster than the larger and gentle glaciers [25–27], as is the case with the Kokthang Glacier. The topographic slope governs the accumulated ice thickness of the tributaries. Empirical estimates of ice thickness from the topographic slope (calculated using Eq. 2) suggest that the ice thickness is much lesser in the eastern tributary. We have derived the ice thickness using slope values at 5 locations along the profiles AA' and BB' (Fig. 2i). The average thickness of the eastern tributary is ~ 4 m, with thinning of the ice sheet at higher elevations (Fig. 3b). As compared to this, the western tributary has a higher average ice thickness, ~ 7.5 m with a thicker terminus (~ 10 m). The topographically controlled variation in accumulated ice thickness may have resulted in the faster recession of the eastern tributary, which was significantly thinner than the western counterpart (Fig. 3b).

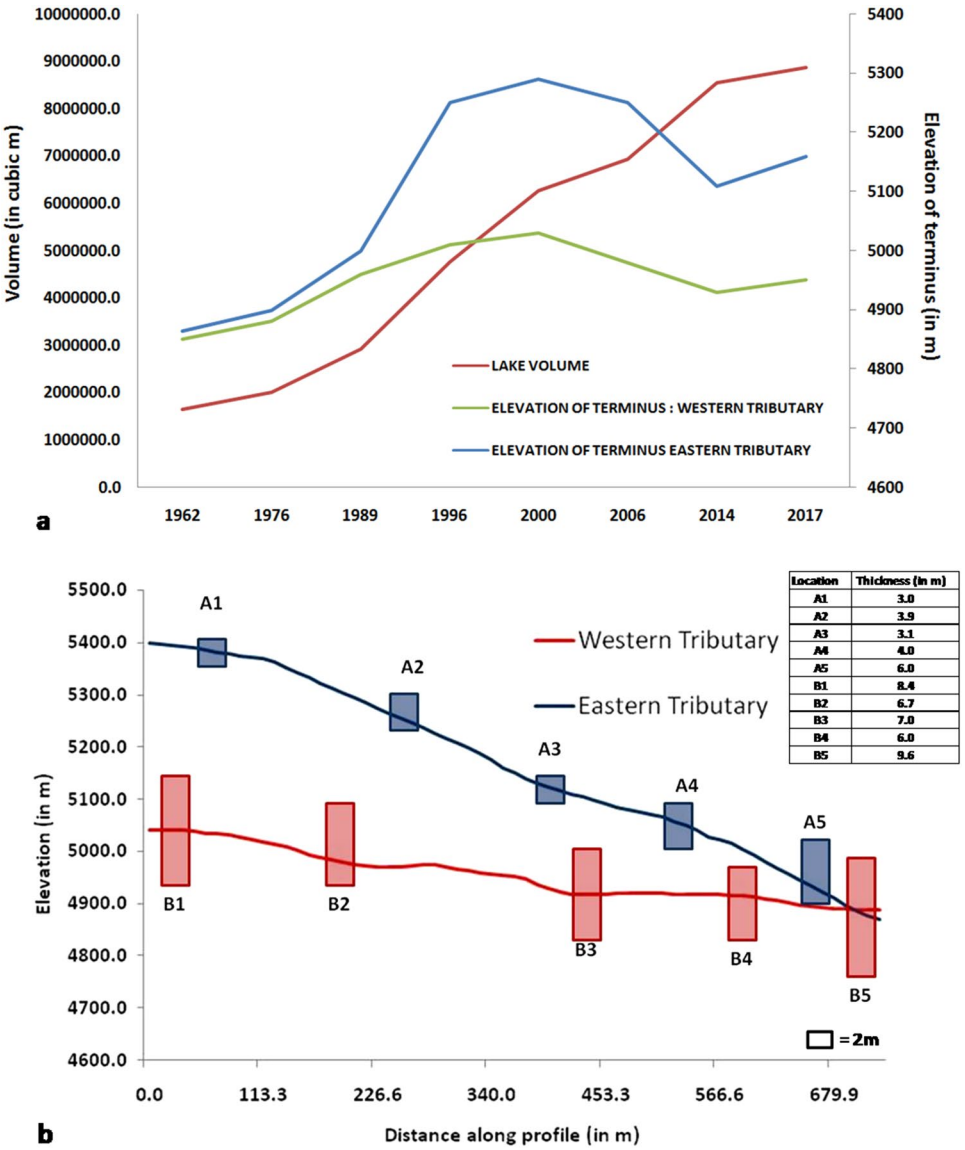

Location	Thickness (in m)
A1	3.0
A2	3.9
A3	3.1
A4	4.0
A5	6.0
B1	8.4
B2	6.7
B3	7.0
B4	6.0
B5	9.6

Fig. 3 **a** Change in elevation of the terminus of eastern and western tributary glaciers and consequent changes in the volume of the lake (estimated from Eq. 1, Huggel et al. [19]), **b** Generalized topographic slope profile AA′ and BB′ (refer Fig. 2i) of eastern and western tributary glaciers along with the thickness of ice accumulation shown by vertical bars. (estimated from Eq. 2, Cooper et al. [20])

5 Conclusion

We have presented preliminary observations regarding the recession and lake formation in the Kokthang Glacier in Sikkim, India. Multi-temporal remote sensing imagery enables the monitoring of glacial dynamics and associated lakes. This, coupled with empirical relationships, provides first-pass quantitative estimates of ice dynamics and lake volumes. The two tributaries of the same glacier can recess differentially being controlled by the underlying topographic slope, which has resulted in differential ice accumulation along with the glacier bodies. The steeper tributary has recessed at a much higher rate and has contributed to the lake enlargement. Due to their dynamic nature, it is now imperative that the glaciers and associated glacial lakes of the Himalaya may be monitored using temporal satellite imagery, spanning over the last five decades. Climatic, as well as non-climatic factors, govern the recession rates and pattern of the glaciers. Lastly, it has to be considered that the observations and quantitative estimates presented in this study are constrained to the spatial resolution and accuracy of the imagery and height accuracy of the DEM. Further, in situ observations are required in this region to precisely quantify the recession rates and lake volumes.

Acknowledgements This paper is an outcome of internal research work in the Geodynamics & Geohazard Division and Mineral exploration & Geoenvironmental Division of Geosciences Group, National Remote Sensing Center (NRSC), Hyderabad. We thank USGS for providing the Corona and Landsat data. We thank Deputy Director (Remote Sensing Applications Area), Associate Director and Director, NRSC, for their support and guidance.

Data availability Data used is available open-source.

Compliance with ethical standards

Conflicts of interest The authors declare that they have no conflict of interest.

References

1. Govindha Raj KB (2010) Remote sensing based hazard assessment of glacial lakes: a case study from Zanskar basin, Jammu and Kashmir. Geom Nat Haz and Risk 1(4):339–347
2. Govindha Raj KB, Kumar KV, Remya SN (2012) Remote sensing-based inventory of glacial lakes in Sikkim Himalaya: semi-automated approach using satellite data. Geom Nat Haz and Risk 4(3):241–253
3. Bahuguna IM, Rathore BP, Brahmbhatt R et al (2014) Are the Himalayan glaciers retreating? Curr Sci 106:5–10
4. Benn DI, Bolch T, Hands K et al (2012) Response of debris-covered glaciers in the Mount Everest region to recent warming, and implications for outburst flood hazards. Earth Sci Rev 114:156–174
5. Fedotov AP, Margold M (2015) Glacier fluctuation in northern and high Asia: historical and methods perspective. Environ Earth Sci 74:1845
6. Patel LK, Sharma P, Fathima TN, Thamban M (2018) Geospatial observations of topographical control over the glacier retreat, Miyar basin, Western Himalaya. India Environ Earth Sci 77(5):190
7. Racoviteanu AE, Williams MW, Barry RG (2008) Optical remote sensing of glacier characteristics: a review with focus on the Himalaya. Sensors 8(5):3355–3383
8. Paul F et al (2013) On the accuracy of glacier outlines derived from remote-sensing data. Ann Glaciol 54(63 Pt 1):171–182
9. Nuimura T, Fujita K, Yamaguchi S, Sharma RR (2012) Elevation changes of glaciers revealed by multitemporal digital elevation models calibrated by GPS survey in the Khumbu region, Nepal Himalayas, 1992–2008. J Glaciol 58(210):648–656
10. Bajracharya, RS, Mool, PK and Shrestha BR, (2006). The impact of global warming on the glaciers of the Himalaya. In Procedings of the International symposium on Geo-disasters, infrastructure management and protection of world heritage sites. 231—242
11. Richardson SD, Quincey DS (2009) Glacier outburst floods from Ghulkin Glacier, Upper Hunza Valley, Pakistan, Geophysical Research Abstracts, 11, EGU2009–12871. EGU General assemblyVienna, Austria
12. Watanabe T (1996) The 1994 Lugge Tsho glacial lake outburst flood, Bhutan Himalaya. Mount Res Develop 16:77–81
13. Martha TR, Roy P, Govindharaj KB, Kumar KV, Diwakar PG, Dadhwal VK (2015) Landslides triggered by the June 2013 extreme rainfall event in parts of Uttarakhand state. India Landslides 12(1):135–146
14. Prakash C, Nagarajan R (2017) Glacial Lake inventory and evolution in Northwestern Indian Himalaya. IEEE J Sel Top Appl Earth Obs Remote Sens 10(12):5284–5294
15. Stokes CR, Popovnin V, Aleynikov A et al (2007) Recent glacier retreat in the Caucasus Mountains, Russia, and associated increase in supraglacial debris cover and supra-/proglacial lake development. Ann Glaciol 46:195–203
16. DeBeer CM, Sharp MJ (2009) Topographical influence on recent changes of very small glaciers in the Monashee Mountains, British Columbia, Canada. J Glaciol 55:691–700
17. Venkatesh TN, Kulkarni AV, Srinivasan J (2012) Relative effect of slope and equilibrium line altitude on the retreat of Himalayan glaciers. The Cryosphere 6(2):301–311
18. Chand P, Sharma MC (2015) Glacier changes in the Ravi basin, northwestern Himalaya (India) during the last four decades (1971–2010/13). Glob, Planet Change
19. Huggel C, Kaab A, Haeberli W, Teysseire P (2002) Remote sensing based assessment of hazards from glacier lake outbursts: a case study in the Swiss Alps. Can Geotech J 39:316–330
20. Cooper APR, Tate JW, Cook AJ (2007) Estimating ice thickness in South Georgia from SRTM elevation data. International Arch Photogramm, Remote Sens Sp Inform Sci 38:592–597
21. Basnett S, Kulkarni A, Shresta DG (2011) Glacier Studies in Sikkim Himalaya. Report number: IISC/DCCC/GLACIER/TR/001/2011. Divecha Centre for Climate Change. https://doi.org/10.13140/RG.2.2.24023.88487
22. Acharya SK, Ray KK (1977) Geology of the Darjeeling-Sikkim Himalaya. Fourth International Gondwana Symposium, Calcutta
23. Bolch T et al. (2007). Automated delineation of debris covered glaciers based on ASTER data, In procedings. of 27th EARSeL Symp 403–410, Millpress, Netherlands. 44
24. Sidjak W, Wheate RD (1999) Glacier mapping of the Illecillewaet Icefield, British Columbia, Canada, using Landsat TM and digital elevation data. Int J Remote Sens 20(2):273–284
25. Pandey P, Kulkarni AV, Venkataraman G (2012) Remote sensing study of snowline altitude at the end of melting season. Chandra-Bhaga basin, Himachal Pradesh, Geocarto Int
26. Scherler D, Bookhagen B, Strecker MR (2011) Hillslope-glacier coupling: the interplay of topography and glacial dynamics in High Asia. J Geophys Res 116:F02019
27. Yao TD, Li ZG, Yang W, Guo XJ, Zhu LP, Kang SC, Wu YH, Yu WS (2010) Glacial distribution and mass balance in the Yarlung Zangbo River and its influence on lakes. Chinese Sci Bull 55(20):2072–2078